

# Using global node-based velocity in random walk particle tracking in variably saturated porous media: application to contaminant leaching from road constructions

Chan-Hee Park · Christof Beyer · Sebastian Bauer ·  
Olaf Kolditz

Received: 4 June 2007 / Accepted: 5 November 2007 / Published online: 22 November 2007  
© Springer-Verlag 2007

**Abstract** Precise and efficient numerical simulation of transport processes in subsurface systems is a prerequisite for many site investigation or remediation studies. Random walk particle tracking (RWPT) methods have been introduced in the past to overcome numerical difficulties when simulating propagation processes in porous media such as advection-dominated mass transport. Crucial for the precision of RWPT methods is the accuracy of the numerically calculated ground water velocity field. In this paper, a global node-based method for velocity calculation is used, which was originally proposed by Yeh (Water Resour Res 7:1216–1225, 1981). This method is improved in three ways: (1) extension to unstructured grids, (2) significant enhancement of computational efficiency, and (3) extension to saturated (groundwater) as well as unsaturated systems (soil water). The novel RWPT method is tested with numerical benchmark examples from the literature and used in two field scale applications of contaminant transport in saturated and unsaturated ground water. To evaluate advective transport of the model, the accuracy of the velocity field is demonstrated by comparing several published results of particle pathlines or streamlines. Given the chosen test problem, the global node-based velocity

estimation is found to be as accurate as the CK method (Cordes and Kinzelbach in Water Resour Res 28(11):2903–2911, 1992) but less accurate than the mixed or mixed-hybrid finite element methods for flow in highly heterogeneous media. To evaluate advective–diffusive transport, a transport problem studied by Hassan and Mohamed (J Hydrol 275(3–4):242–260, 2003) is investigated here and evaluated using different numbers of particles. The results indicate that the number of particles required for the given problem is decreased using the proposed method by about two orders of magnitude without losing accuracy of the concentration contours as compared to the published numbers.

**Keywords** Velocity approximation · Particle tracking · Random walk · Transport in porous media · Contaminant leaching from road constructions

## Introduction

Tracing particles within the Lagrangian framework to describe advective–diffusive transport in porous media has received much attention in the literature over the past several decades. As the flow velocity is of great importance in modeling transport accurately, research has been conducted to meet the need for obtaining accurate velocity fields mainly governed by Darcy’s law in subsurface systems (Chavent and Roberts 1991; Cirpka et al. 1999; Cordes and Kinzelbach 1992; Hoteit et al. 2002; Matringe et al. 2006; Mose et al. 1994; Yeh 1981).

Because the standard finite element method (FEM) estimates the flow velocity on the element level using the Darcy equation, local heads and parameters, discontinuities of the flow velocity may occur at the element or cell

---

C.-H. Park (✉) · O. Kolditz  
Department of Environmental Informatics,  
Helmholtz Centre for Environmental Research, UFZ,  
Permoserstrasse 15, 04318 Leipzig, Germany  
e-mail: chanhee.park@ufz.de

C. Beyer  
Center for Applied Geoscience, University of Tuebingen,  
Sigwartstr. 10, 72076 Tuebingen, Germany

S. Bauer  
Geoscience Institute, University of Kiel,  
Ludewig-Meyn-Str. 10, 24118 Kiel, Germany

boundaries. To resolve these discontinuities, several methods have been introduced. Using the same structure of the standard FEM as in groundwater flow, Yeh (1981) proposed to solve Darcy's law for the velocity field globally at nodal points using an FEM. Cordes and Kinzelbach (1992) provided a post-processing methodology for element-based flow velocities based on flux-continuous control volumes surrounding a node and conserving local mass balance. On the other hand, the mixed or mixed-hybrid FEM forms up the pressure, and the Darcy equation is used to solve for pressure and the velocity field simultaneously. These methods are able to produce accurate streamlines, regardless of the degree of heterogeneity and also in block heterogeneous systems (Ackerer et al. 1996; Cordes and Kinzelbach 1996; Durlinsky 1994; Mose et al. 1994). Recently, higher-order mixed FEMs have also been provided to obtain more accurate streamlines for steady state flow (Matringe et al. 2006).

On tracing pathlines for transient flow, Cheng et al. (1996) developed a multi-dimension particle tracking technique to solve transport under unsteady flow conditions. Bensabat et al. (2000) provided an adaptive-pathline based particle tracking for the Eulerian-Lagrangian method in solving transport. In these works, velocity fields are computed at nodes instead of element or cell edges. In contrast, the velocity field is estimated at edges in all mixed or mixed-hybrid FEMs. Recently, Haegland et al. (2007) reconstructed velocities obtained along edges to nodes through corner-velocity interpolation and demonstrated improved streamlines and time-of-flight on irregular grids. They found that the node-based velocity method eliminates the influence of cell geometries on the velocity field, and thus were able to accurately reproduce uniform flow in 3D.

As particle tracking methods are suited for advection dominated transport and the Eulerian method is suited in the case of diffusive transport, both methods can be combined in the form of the Eulerian-Lagrangian methods. Using an Eulerian-Lagrangian method, Oliveira and Baptista (1998) showed that due to the failure of mass balance during the combination of the methods, severe tracking errors can be introduced and therefore developed an accurate tracking algorithm. Alternatively, solving advection and diffusion transport problems fully by the Lagrangian method such as the random walk particle tracking (RWPT) methods can preserve mass balance locally and globally. However, oscillations due to the random number generation exist by the nature of the method.

Although the RWPT method has not been used widely for multi-phase flow, Delay et al. (2005) emphasized promising suitability of the method for modeling solute transport in the vadose zone because strong variations of velocity in the vadose zone can easily be handled in a

flexible way using this approach. The RWPT method has also little numerical difficulties restricted by the Peclet number criterion (Hassan and Mohamed 2003; Salamon et al. 2006). With strong variations of velocity, anomalous transport can easily occur. Since anomalous transport is observed in the system in which a variable velocity field is envisioned as particles via different paths moving spatially changing velocities (Cortis and Berkowitz 2005).

This paper, therefore, demonstrates the use of the global node-based method for estimation of the ground water flow velocity field based on the standard FEM. A global node-based method for flow velocity calculation, as originally proposed by Yeh (1981), is extended to unstructured grids and unsaturated ground water, and the computational efficiency is enhanced. This method has been recently used for modeling of flow and transport in subsurface systems (Jang and Aral 2007; Park and Aral 2007), but the accuracy in tracing pathlines and in RWPT has not yet been evaluated. Thus, the objective of the paper is to introduce and investigate the accuracy of a global node-based method for flow velocity determination and to apply the method for RWPT in two field scale applications in variably saturated porous media. After starting the governing equations for RWPT, the formulation of the global node-based method is provided. To evaluate the applicability and accuracy of the proposed method for advective or advective–diffusive transport in variably saturated media and under transient flow conditions, the method is tested against published benchmark problems, a benchmark for unsaturated transient transport as well as compared to an analytical solution. Efficiency in terms of the numbers of particles required is assessed by comparing to results recently published. Finally, the proposed method is applied in a study on contaminant leaching from demolition waste, which is reused as base layers in road constructions. The RWPT model is used to characterize the spatial variability of unsaturated flow and transport patterns in a noise protection dam and a road dam scenario. Based on the simulated flow fields, contaminant leaching from the road constructions to the groundwater surface is modeled for both scenarios accounting for biodegradation and rate limited sorption, which is governed by intraparticle diffusion kinetics. The temporal development of breakthrough concentrations at the groundwater surface for three different organic contaminants (weakly, moderately and strongly sorptive) is presented and compared for both scenarios, highlighting the dominant role of the respective dam hydraulics on the transport behavior.

## Methods

This section consists of governing equations, numerical formulation of the global node-based velocity estimation,

and velocity interpolation in elements needed in developing the proposed RWPT method. The governing equations are mainly composed of flow and transport equations. The flow system is determined by the FEM model, whereas the transport system is solved by the RWPT model. Therefore, obtaining pressure or saturation ratio of Richards flow (i.e. flow in variably saturated porous media) is independent of the RWPT model. With the known pressure distribution, velocity is obtained by the method of global node-based velocity. However, velocity interpolation from the known velocity fields is necessary for the RWPT model to determine transport.

### Governing equations

The governing equation for groundwater flow under transient conditions is given by (Bear 1972)

$$S_h \frac{\partial h}{\partial t} = \nabla \cdot (\mathbf{K} \nabla h) + Q \tag{1}$$

where  $S_h (L^{-1})$  is specific storativity,  $h (L)$  is the hydraulic head, given as the sum of elevation  $z (L)$  and the pressure head  $\psi (L)$ ,  $t (T)$  is time,  $\mathbf{K} (LT^{-1})$  is the tensor of hydraulic conductivity,  $Q (T^{-1})$  is a source or sink term, and  $\nabla$  is the differential operator. For unsaturated conditions  $\mathbf{K}$  is a function of the pressure head  $\psi$ , which itself depends on the volumetric water content  $\theta (-)$  of the porous medium. The governing equation of flow for unsaturated conditions is the so-called Richards equation, which exists in three main forms with  $\psi$ ,  $\theta$  or both quantities as dependent variables (Jury et al. 1991). Equation (2) is the  $\psi$ -based form of the Richards equation (Freeze and Cherry 1979).

$$C_w(\psi) \frac{\partial \psi}{\partial t} = \nabla \cdot (\mathbf{K}(\psi) \nabla \psi) + \frac{\partial \mathbf{K}(\psi)}{\partial z} + Q \tag{2}$$

where  $C_w(\psi)$  is the water capacity function defined by  $d\theta/d\psi$  and with  $z$  positive in a downward direction.

The advection–dispersion equation governing transport of a conservative solute in porous media can be written as (Bear 1979)

$$\frac{\partial C}{\partial t} = -\nabla \cdot (\mathbf{V}C) + \nabla \cdot (\mathbf{D} \nabla C) \tag{3}$$

where  $C$  is the concentration ( $ML^{-3}$ ),  $\mathbf{V}$  is the pore velocity vector ( $LT^{-1}$ ),  $\mathbf{D}$  is the hydrodynamic dispersion tensor ( $L^2 T^{-1}$ ), and  $\nabla$  is the differential operator.

The modified velocity (Kinzelbach 1986) and the hydrodynamic dispersion tensor (Bear 1979) are expressed in componential notation as

$$V_i^* = V_i + \sum_{j=1}^3 \frac{\partial D_{ij}}{\partial x_j} \tag{4}$$

$$D_{ij} = \alpha_T |\mathbf{V}| \delta_{ij} + (\alpha_L - \alpha_T) \frac{V_i V_j}{|\mathbf{V}|} + D^d \tau_{ij} \tag{5}$$

where  $\delta_{ij}$  is the Kronecker symbol,  $\alpha_L$  is the longitudinal dispersivity ( $L$ ),  $\alpha_T$  is the transverse dispersivity ( $L$ ),  $D^d$  is the molecular diffusion coefficient ( $L^2 T^{-1}$ ),  $\tau_{ij}$  is the tortuosity tensor (-), and  $V_i$  is the component of the mean pore velocity in the  $i$ th direction.

For unsaturated conditions the total solute flux in the water phase is described by

$$\frac{\partial \theta C}{\partial t} = -\nabla \cdot (\mathbf{q} \theta C) + \nabla \cdot (\theta \mathbf{D}_e \nabla C) \tag{6}$$

where  $\mathbf{q} (LT^{-1})$  is the Darcy flux vector of the effective hydrodynamic dispersion tensor  $\mathbf{D}_e$  is used, as besides  $D^d$  also  $\alpha_L$  and  $\alpha_T$  depend on  $\theta$  (Bear, 1979).

In (3) and (6) anisotropic molecular diffusion can be handled via the tortuosity tensor. Note that there is clear distinction between hydrodynamic dispersion and molecular diffusion.

The stochastic differential equation for particle position at a new time level  $t + \Delta t$  equivalent to (3) in three-dimensional problems can be written as (Hassan and Mohamed 2003; LaBolle et al. 1996; Tompson and Gelhar 1990)

$$\begin{aligned} x_{t+\Delta t} &= x_t + \left( V_x(x_t, y_t, z_t, t) + \frac{\partial D_{xx}}{\partial x} + \frac{\partial D_{xy}}{\partial y} + \frac{\partial D_{xz}}{\partial z} \right) \Delta t \\ &\quad + \sqrt{2D_{xx}\Delta t}Z_1 + \sqrt{2D_{xy}\Delta t}Z_2 + \sqrt{2D_{xz}\Delta t}Z_3 \\ y_{t+\Delta t} &= y_t + \left( V_y(x_t, y_t, z_t, t) + \frac{\partial D_{yx}}{\partial x} + \frac{\partial D_{yy}}{\partial y} + \frac{\partial D_{yz}}{\partial z} \right) \Delta t \\ &\quad + \sqrt{2D_{yx}\Delta t}Z_1 + \sqrt{2D_{yy}\Delta t}Z_2 + \sqrt{2D_{yz}\Delta t}Z_3 \\ z_{t+\Delta t} &= z_t + \left( V_z(x_t, y_t, z_t, t) + \frac{\partial D_{zx}}{\partial x} + \frac{\partial D_{zy}}{\partial y} + \frac{\partial D_{zz}}{\partial z} \right) \Delta t \\ &\quad + \sqrt{2D_{zx}\Delta t}Z_1 + \sqrt{2D_{zy}\Delta t}Z_2 + \sqrt{2D_{zz}\Delta t}Z_3 \end{aligned} \tag{7}$$

where  $x$ ,  $y$ , and  $z$  are the coordinates of the particle location,  $\Delta t$  is the time step, and  $Z_i$  is a random number whose mean is zero and variance is unit.

### Node-based velocity

In the standard FEM, hydraulic head or pressure is calculated by solving the flow equation. With solved hydraulic head, velocity is obtained using the Darcy equation.

$$\mathbf{q} = \phi \mathbf{V} = -\mathbf{K}(S) \nabla h \tag{8}$$

where  $\mathbf{q}$  is the Darcy velocity ( $LT^{-1}$ ),  $\phi$  is the porosity (-),  $\mathbf{V}$  is the pore velocity,  $\mathbf{K}$  is the hydraulic conductivity ( $LT^{-1}$ ),

which under unsaturated conditions is dependent on the saturation ratio  $S(-)$ , and  $h$  is the hydraulic head ( $L$ ). Normally, velocity is estimated in the center of the element using the hydraulic head values at the surrounding nodes. This creates discontinuities in the velocity along elemental boundaries if heterogeneities are present, because velocity estimation is based solely on the information obtained from the element of interest.

To resolve discontinuities and to keep global information of hydraulic head in the Darcy law, subject to boundary and initial conditions the Darcy velocity is solved using the Galerkin method (Yeh 1981)

$$\int_{\Omega} (\mathbf{q} + \mathbf{K}\nabla h)\omega \, d\Omega = 0 \quad (9)$$

where  $\Omega$  is the model domain and  $\omega$  is a trial function.

The element matrix  $M$  and vector  $q$  corresponding to (9) formulate as

$$[M_{ij}] \{q_j\} = \{H_i\} \quad (10)$$

where

$$M_{ij} = \int_{\Omega^e} \omega_i \omega_j \, d\Omega^e \quad (11a)$$

where  $\Omega^e$  is the element domain and

$$H_i = - \int_{\Omega^e} [\mathbf{K}\nabla(\omega_j h_j)] \omega_i \, d\Omega^e \quad (11b)$$

Except for  $q$ , all values are known once the hydraulic head distribution is solved. Then, Eq. (11a) represents a mass matrix that can be solved consistently or lumped. Note that the global matrix formed from (11a) is constant for a given discretized domain so that the matrix needs not be assembled repetitively once formulated. Only the vector  $\{H_i\}$  changes subject to the head distribution. This additionally reduces the computational burden introduced by solving for velocity component-wise, depending on the number of dimensions. Because of a well-defined hydraulic head distribution used in  $\{H_i\}$  after solving the flow equation, computation time for each directional velocity is much shorter than that for hydraulic head for the test problems provided in this paper.

In comparison to other methods, such as the mixed or mixed-hybrid finite element, the finite difference or the finite volume methods, it is worthwhile to mention that global mass conservation is achieved for each component over the whole problem domain by applying appropriate Dirichlet and Neumann type boundary conditions to represent the fluxes. The physical meaning of these boundary conditions can be seepage or rainfall infiltration or impervious boundaries. No local mass conservation at the

element level is guaranteed due to the nature of the standard FEM. Therefore, this method is affected by local mass balance errors occurring in the hydraulic head calculation e.g. in the case of highly heterogeneous media. An evaluation of the errors that may occur is provided by evaluating the benchmark test problems.

Further advantages of the global velocity estimation are as follows:

1. Flexibility for obtaining subsequent velocities at edges or faces.
2. The order of the approximation function for velocities along the edge or the surface can easily be varied.
3. Feasibility for existing finite element codes due to the similarity to the standard FEM.
4. Easy adaptation for unstructured grids in all dimensions.

#### Velocity interpolation in elements

Whether the velocity field is obtained using numerical methods on nodes, edges, faces or midpoints of elements, an accurate interpolation of the velocity from the known points to the particle position should be guaranteed by an appropriate interpolation scheme. For velocity solved on edges or faces, the Pollock method (Pollock 1988) has been used with popularity (Cordes and Kinzelbach 1992; Haegland 2003; Prevost et al. 2002).

As for nodal velocity approximation, nodal velocity can be converted to edge velocity as in Prevost (2000) or by similar compatible methods. In this work, the global node-based velocity fields is converted to edge-centered velocity fields in order to use Pollock's method for structured elements (Pollock 1988). In this conversion process, an arithmetic average method over two ending points of each edge is used with equal distance weight for two velocities normal to the common edge of two adjacent elements.

On the other hand, using Pollock's method for interpolation for unstructured elements requires isoparametric transformation from physical space to reference space. Depending on the number of dimensions, the inverse functions of linear, bilinear or trilinear functions are required, and the vector transformation should also be made accordingly using the Piola transform (Brezzi and Fortin 1991). Then, the time of flight needed for a particle from entry to exit point of the element is in general computed for tracing streamlines. Note that this method is strictly constrained by the time of flight for steady state flow. Time of flight for unsteady flow should complicate Pollock's method and leads solely to numerical integration. In case that particles are traced under unsteady state flow

system, interpolation at any location inside of elements is necessary.

**Benchmarking**

The proposed RWPT method is implemented in the open source scientific software GeoSys/RockFlow (GS/RF) (Kolditz et al. 2007a, b) and tested with several benchmark test problems. In terms of transport mechanisms for the proposed RWPT method, first advective transport is tested for accurate velocity fields. Second dispersive (or diffusive) transport with the fixed uniform advection is compared against an analytical solution, and the results previously published by others. Finally, advection and dispersion together are also compared with the results obtained by the FEM model. These tests are conducted in various medium types (fractured and porous media) and summarized in Table 1.

For evaluating the accuracy of the RWPT method for variably saturated porous media, examples are focused for the accuracy of the velocity calculation in heterogeneous media and diffusion in homogeneous media. To test the RWPT model in unsaturated porous media, additional results obtained by solving the experiment from Warrick et al. (1971) are provided in this paper. The pressure fields obtained for unsaturated flow have been compared against results obtained with MIN3P (Mayer et al. 1999) and HYDRUS (Šimůnek et al. 2005). The results are in good agreement as reported in Kolditz et al. (2007a, b).

**Benchmarking advective transport in heterogeneous saturated media**

The test problem is taken from Mose et al. (1994) and formulated to examine the accuracy of velocity fields in highly heterogeneous media. A unit square domain is discretized using  $40 \times 40$  quadrilateral elements. The maximum material contrast in hydraulic conductivity is set

to be four orders of magnitude as detailed in Fig. 1a. Groundwater flows from top to bottom because of the pressure gradient assigned by the two head boundary conditions along the top and bottom of the model domain. Depending on the configuration of the four different materials, flow patterns vary. For the given inhomogeneous medium, the solution obtained by the global node-based velocity method shows very good agreement with the exact solution obtained by solving stream functions using a much higher grid density (Mose et al. 1994). In general, the global node-based velocity method produces smoother streamlines than the mixed or mixed-hybrid FEM (Fig. 1b, c).

**Benchmarking advective–diffusive transport in homogeneous saturated media**

This example was taken from Hassan and Mohamed (2003) to test advective–diffusive transport in a homogeneous two-dimensional aquifer of  $100 \text{ m} \times 60 \text{ m}$  where a uniform velocity field is held constant at  $0.5 \text{ m d}^{-1}$  in the  $x$  direction. The hydraulic conductivity is set as  $10^{-5} \text{ m d}^{-1}$  and the head gradient of 1 in the  $x$  direction is set by assigning two constant head boundary conditions along both the left and right sides. Dispersivity is chosen to be isotropic with a length of  $0.1 \text{ m}$  in the longitudinal as well as the transverse direction. The initial source load is applied to an area with dimensions of  $0.1 \text{ m} \times 0.1 \text{ m}$  to have an initial concentration of  $C_0 = 1 \text{ kg m}^{-3}$ . Figure 2 provides a schematic description of the test problem. The domain is discretized with quadrilateral elements of  $0.5 \text{ m} \times 0.5 \text{ m}$ . The same grid density is also used for converting particle distributions to element concentrations.

The stated problem can be solved with the analytical solution provided by Ogata and Banks (1961). This allows evaluating the computational accuracy of the solution in terms of particle density. The concentration contours for the different numbers of particles and for transport times of 20, 40, and 60 days are compared to the analytical solution

**Table 1** Benchmarks for the RWPT method (Park et al. 2007)

Characteristics	Transport	Medium type	Reference
Divergent and convergent flow	Advection	Homogeneous	Cordes and Kinzelbach (1992)
Flow in dipole of discharging and recharging wells	Advection	Homogeneous	Cordes and Kinzelbach (1992)
S shape flow	Advection	Two highly contrasted composite media	Matringe et al. (2006)
Diverse flow	Advection	Heterogeneous	Mose et al. (1994)
Uniform flow	Advection and diffusion	Homogeneous	Ogata and Banks (1961)
Diverse flow	Advection and diffusion	Heterogeneous	

**Fig. 1** **a** Hydraulic conductivity distribution for the  $1\text{ m} \times 1\text{ m}$  domain, **b** the exact solution of the streamlines obtained from the stream function approximation with a  $320 \times 320$  mesh from Mose et al. (1994) and **c** streamlines obtained from  $40 \times 40$  grid

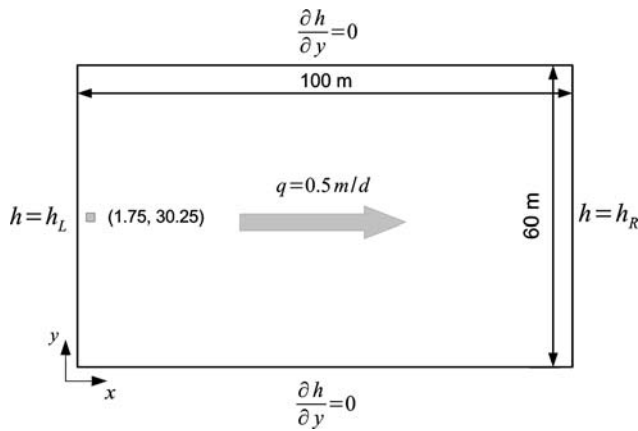
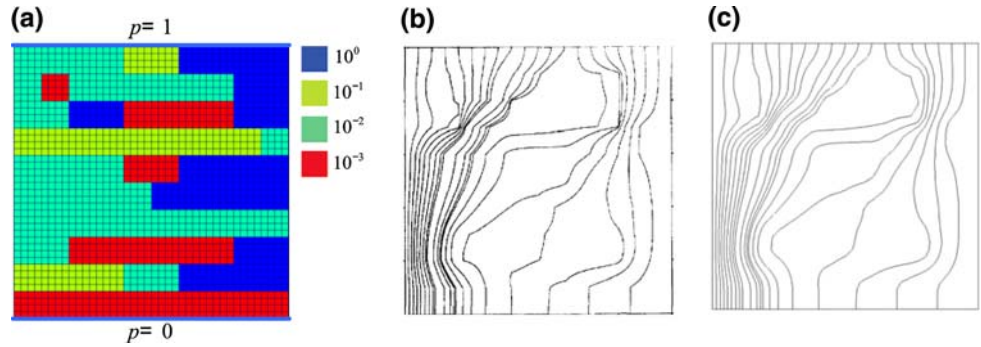


**Fig. 2** Schematic description of the two-dimensional aquifer and the boundary conditions of the flow system

in Fig. 3. As the number of particles increases, the result of the RWPT method shows better agreement with the analytical solution. The best agreement is found to be for 50,000 particles among the chosen numbers of particles. This is significantly less than the number of particles reported by Hassan and Mohamed (2003), who found that up to 2.5 million particles were necessary to achieve smoothness of the solution due to oscillations around the contours. In general, the degree of oscillations along the contours decreases with increasing number of particles. As the oscillations observed here are much smaller than that reported by Hassan and Mohamed (2003), the present method allows to significantly reduce the number of particles required for a smooth solution by about two orders of magnitude in comparison to their method.

To quantify the errors of concentrations computed by the RWPT method with respect to the analytical solution, the sum of squared concentration differences is computed between the analytical solution and the numerical simulation from all cells. Results for 60 days of simulation time are shown in Fig. 4, where both measures are plotted against the number of particles used. As can be seen, the deviation between the analytical and the numerical results decreases significantly, if the number of particles used is

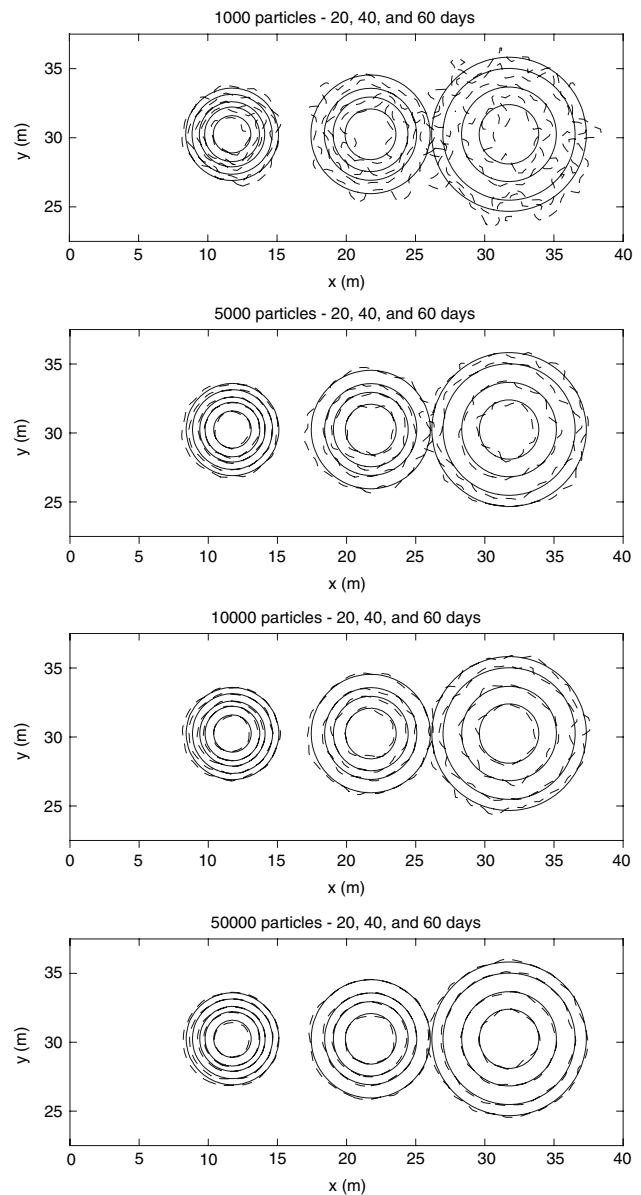
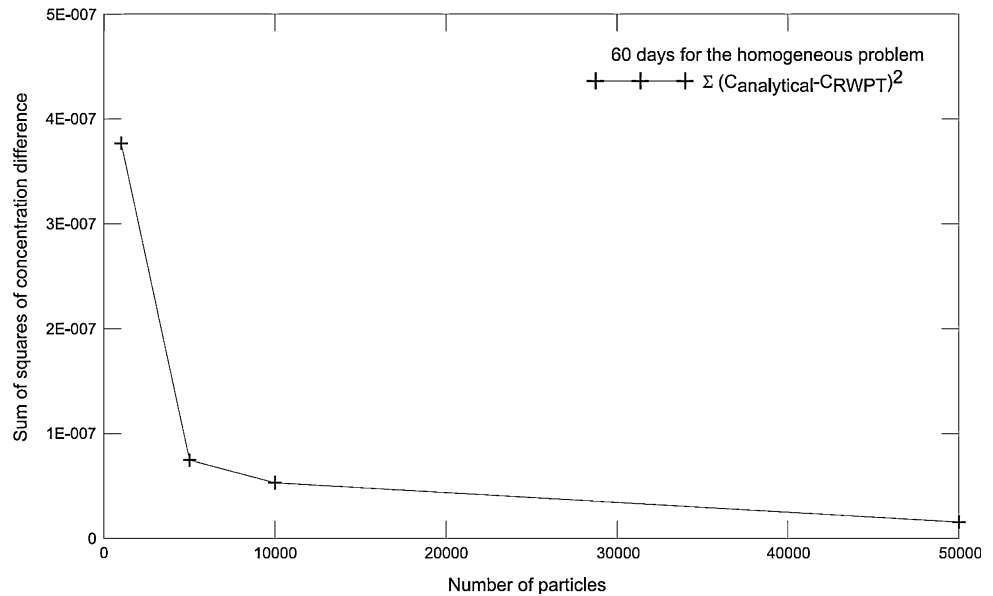


**Fig. 3** Concentration contours converted from the particle distributions for 1,000, 5,000, 10,000, and 50,000 particles: The *solid line* is the analytical solution, the *dotted line* is the RWPT result. *Contour lines* are shown for  $C = 2.6e^{-4}$ ,  $1.6e^{-4}$ ,  $1.0e^{-4}$ , and  $4e^{-5}$ [-]

**Fig. 4** Sum of squares of concentration difference to the analytical solution of each cell for the homogeneous medium



increased from 1,000 to 10,000. Because of the stochastic nature of the dispersive step, concentration approximation converted from the particle distribution requires a certain number of particles. In general, more particles give more accurate concentration distribution. For the test case shown here, the finding is that 50,000 particles are required to reproduce the concentration contours with high accuracy comparable to the results produced by Hassan and Mohamed (2003). However, 10,000 particles seem sufficient to obtain a good average mass distribution (Fig. 4).

**Benchmarking advective–diffusive transport in variably saturated porous media**

To benchmark mass transport in variably saturated media, the soil experiment of Warrick et al. (1971) is selected for unsaturated flow and transport. The comparison between the numerical results and the experimental measurement can be found in Kolditz et al. (2007a) for both flow and transport. In the comparison, the results are obtained from the finite element model, which is verified against numerous test cases for unsaturated flow (Kolditz et al. 2007a).

The 2 m high soil column is installed to have the top open to atmosphere ( $P_{cap} = 0 Pa$ ). The bottom of the column has a capillary pressure ( $P_{cap} = 21,500 Pa$ ). While these fixed pressure boundary conditions are used in the flow equation with an initial saturation of 45.5% over the whole column, an inactive tracer is injected for 100 s on the top of the column (see Fig. 5). Details on parameters used in the numerical simulation are summarized in Table 2.

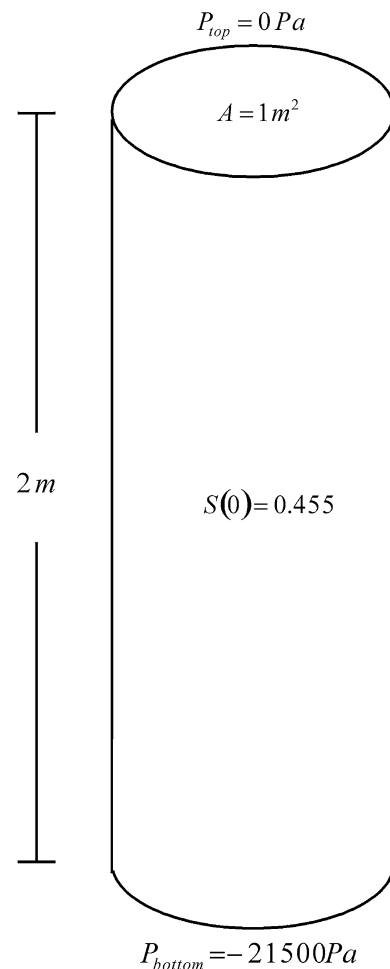


**Fig. 5** Initial conditions and boundary conditions for the column experiment by Warrick et al. (1971)

**Table 2** Parameters for flow and mass transport in the Warrick et al. (1971) benchmark

Parameter	Value
Porosity	0.38
Permeability	$4.46 \times 10^{-13} \text{ m}^2/\text{s}$
Molecular diffusion coefficient of tracer	$6.0 \times 10^{-10} \text{ m}^2/\text{s}$
Mass source influx	$1 \text{ kg m}^{-3}$ for 100 s at the top

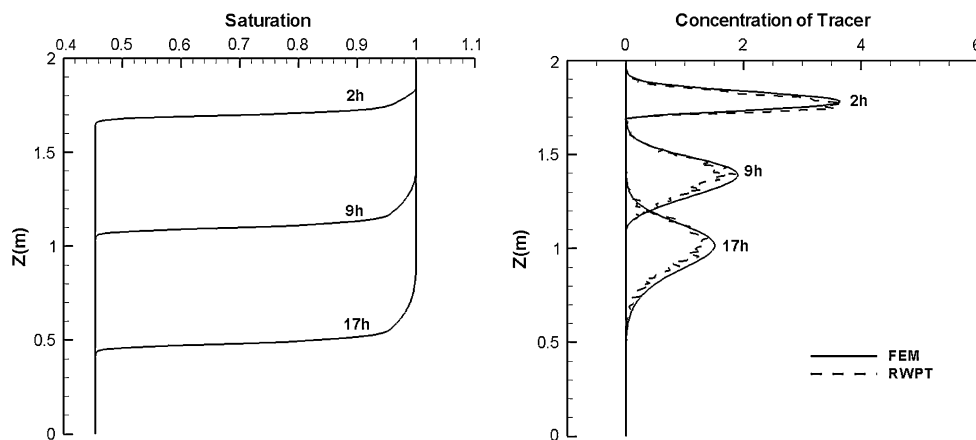
As pressure is calculated and used for solving the global node-based velocity along the column, the resulting mass transport can be solved with transient velocity fields. In addition, the temporal spatial development of soil saturation in the column is obtained from the pressure solution determined by the FEM. In solving mass transport, the FEM and RWPT models are used for comparison purpose. Figure 6 shows saturations and two concentration contours from the two different models at 2, 9, and 17 h. Both concentration contours are in good agreement in terms of peaks and shapes of trace development in the column, indicating that the proposed method is capable of solving mass transport in variably saturated media accurately. Unlike the FEM, the contours from the RWPT model are subject to subtle oscillation. This oscillation can be reduced by increasing the number of particles as shown in Fig. 3 for saturated flow. Nevertheless, the oscillation is inherent to the RWPT method.

## Applications

The RWPT method is applied in a study on the environmental impact of secondary materials in road constructions on groundwater quality (Beyer et al. 2007). In this study, the leaching of organic contaminants from demolition waste, which is reused for base layers in a noise protection dam and a road dam, was assessed by performing numerical

reactive transport simulations using GS/RF coupled to the Lagrangian stream tube model SMART (Finkel et al. 1999). The RWPT method is applied for the hydraulic characterization of the road constructions via probability density functions (pdf)  $g(\tau, x) (T^{-1})$  of the travel time  $\theta (T)$  of a non-reactive passive tracer along a stream tube. The conceptual models of the noise protection dam and the road dam are depicted in Fig. 7a, b. Both constructions consist of layered composite porous materials with strongly contrasting hydraulic properties on top of a sandy podzol soil with low organic carbon content. The geometry of the road dam (Fig. 7b) is comparable to that of a typical smaller four-lane German Autobahn. The horizontal layering of materials used within the dam as well as the soil horization below the road dam and the noise protection dam, however, are simplified. Basis for the application of the RWPT method in the unsaturated composite media is the derivation of the Eulerian steady state velocity fields on the respective finite element grids (see Fig. 8a, b) using the flow equation for unsaturated conditions, i.e. the so-called Richard's equation.

Both two-dimensional models exhibit complex unsaturated flow patterns. The velocity vectors at the finite element mesh nodes (Fig. 8a, b) clearly show strong capillary barrier effects along the sloped boundaries of the material layers which cause a concentration of the seepage fluxes on top of the demolition waste and generation of lateral runoff, almost completely bypassing the demolition waste. To derive the travel time pdf  $g(\theta, x) (a^{-1})$  of the passive tracer in each material layer of both models, an instantaneous tracer source represented by 10,000 particles was evenly distributed along each upper material layer boundary. The particles were transported within the unsaturated flow fields employing the RWPT method.  $g(\theta, x)$  was then obtained by registering the particles breakthrough times at each respective lower material layer boundary. The results were checked against travel time distribution derived from finite element mass transport

**Fig. 6** Saturation ratio and tracer concentration at 2, 9, and 17 h for FEM and RWPT



**Fig. 7** Conceptual models of the noise protection dam (a) and the road dam (b)

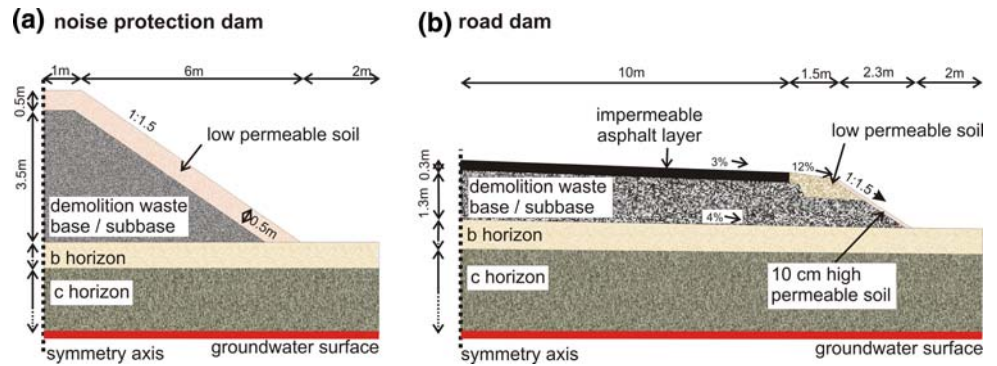
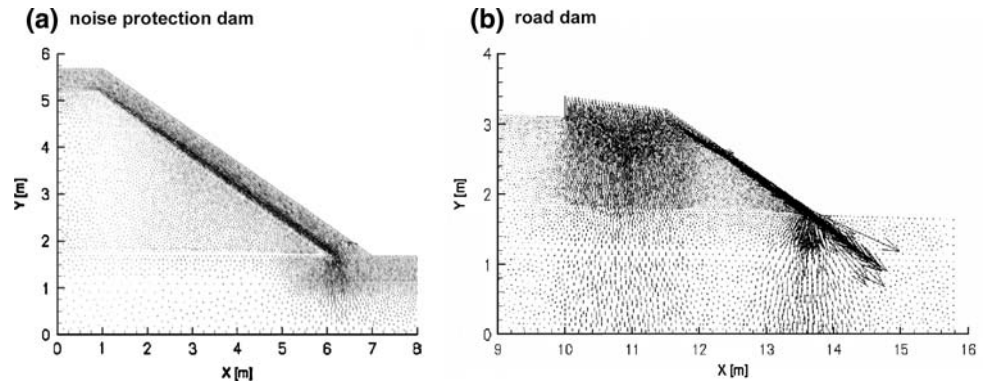


**Fig. 8** Velocity vectors at the finite element nodes for the noise protection dam (a) and a cut out of the road dam (b)



simulations with the classical advection–dispersion Eq. (1). Figure 9 shows a comparison of the resulting pdf  $g(\theta, x)$  for the RWPT-method and the finite element mass transport simulation for the base layer of the noise protection dam (see Fig. 7a). Despite the relatively simple composition of the noise protection dam, the pdf pattern shows distinct extremes—early peaking and a long tailing, i.e. a fraction of approximately 10% of the particles is transported extremely rapid (within weeks) through the demolition waste layer, whereas the remaining fraction experiences comparably long residence times (several months to years). In general, the results from both methods show a very good agreement in the timing of peak arrivals and their relative magnitudes. Also, the tails of the pdf correspond well.

Figure 10 presents the pdf  $g(\theta, x)$  derived with the RWPT method for the road dam base layer and the subsoil. Both layers show a distinctively different transport behavior. For the demolition waste in the road dam base layer, breakthrough of a large fraction of the passive tracer is immediate as indicated by the peak of approximately 66% occurring after a few weeks only. This rapid transport component is a consequence of the flow focusing at the foot of the embankment, clearly obvious in Fig. 8b. For other parts of the domain, transport velocities are slower causing the long tailing of the pdf. In the subsoil the very high transport velocities observed for the demolition waste are somewhat dampened. Here, the pdf peak travel time is

observed after approximately 240 days, whereas the tailing of the  $g(\theta, x)$  is somewhat increased as compared to the base layer pdf.

In addition to the pdf, the particle distribution after 2 years is used to obtain a snapshot of concentration contours of the particles. In the conversion process, a unit area is empirically chosen to be 0.2 m × 0.2 m. The

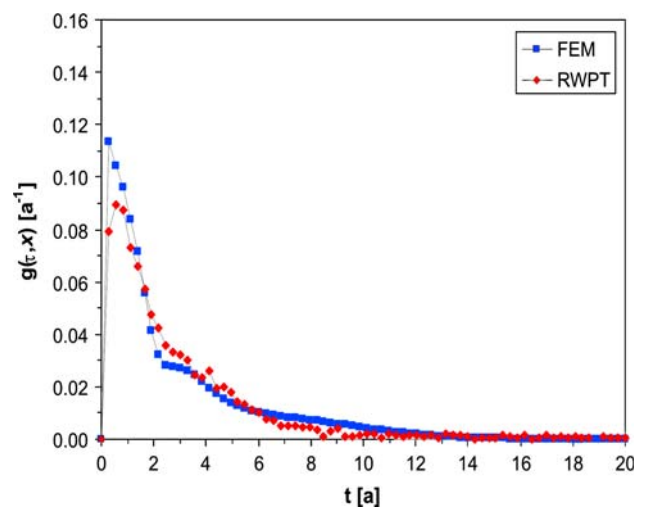


**Fig. 9** Travel time distributions (pdf)  $g(\theta, x)$  for the demolition waste base layer of the noise protection dam example calculated with standard FEM and RWPT

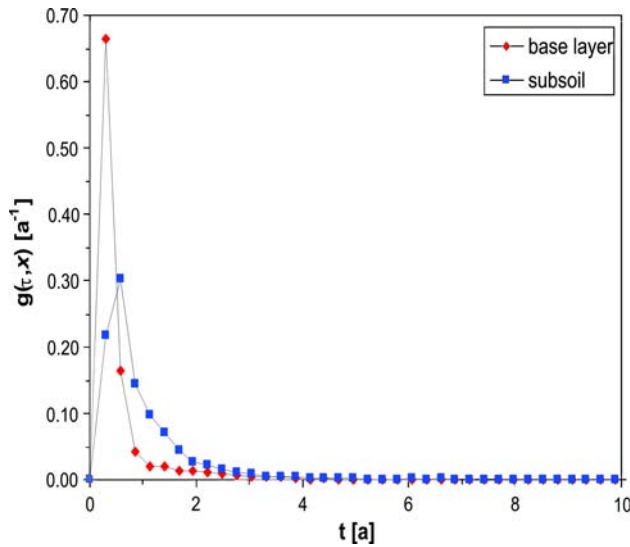


**Fig. 10** Travel time distributions (pdf)  $g(t, x)$  for the demolition waste base layer and the subsoil of the road dam example

concentration contours after 2 years for the noise protection dam is provided in Fig. 11.

Figure 12 presents breakthrough curves for three different sorbing contaminants, naphthalene, phenanthrene and a sum parameter  $\Sigma$  15EPA-PAH for the 15 most relevant polyaromatic hydrocarbons (PAHs) according to the US Environmental Protection Agency (EPA). The breakthrough curves were calculated with RF/GS + SMART based on the pdfs shown above. Sorption kinetics were in each case modeled by intraparticle diffusion kinetics (Grathwohl 1998). For each of the three contaminants transport was calculated with and without biodegradation. The breakthrough curves represent spatially averaged breakthrough concentrations along the groundwater surface

at the lower model boundaries of the noise protection dam and the road dam, respectively.

The breakthrough curves for the noise protection dam are shown in Fig. 12a. Clearly visible is the increasing retardation from naphthalene (weakly sorbing) over phenanthrene (medial sorbing) to  $\Sigma$  15EPA-PAH (strongly sorbing), for which both the peak breakthroughs are not yet reached after 500 years of simulation time. Accounting for biodegradation reduces breakthrough concentrations significantly for all three compounds by about 95%. In contrast to this, contaminant breakthrough is significantly higher and much earlier for the road dam (Fig. 12b), which is caused by higher flow velocities in the dam structure. These are a consequence of higher average infiltration rates in comparison to the noise protection dam due to surface run off from the road asphalt layer which is infiltrating along the side-strip and the embankment of the road dam. Due to the resulting lower residence times of the contaminants in the unsaturated zone, breakthrough concentrations at the groundwater surface are high, even if contaminant degradation is accounted for in the simulation.

## Summary and conclusions

In this paper, the RWPT model that uses the global node-based velocity calculation is demonstrated. The method is tested for the accuracy of velocity using the various benchmark problems. The accuracy of the calculated velocity field for the chosen problems is found to be compatible with the CK method (Cordes and Kinzelbach 1992). In addition, the method is flexible for various shapes of elements that include structured and unstructured elements. However, the velocity interpolation for any arbitrary position from the known

**Fig. 11** Concentration contours converted from the particle distribution at 2 years of the simulation. The numbers in the scale column represent the number of particles in a unit square of  $0.2 \text{ m} \times 0.2 \text{ m}$

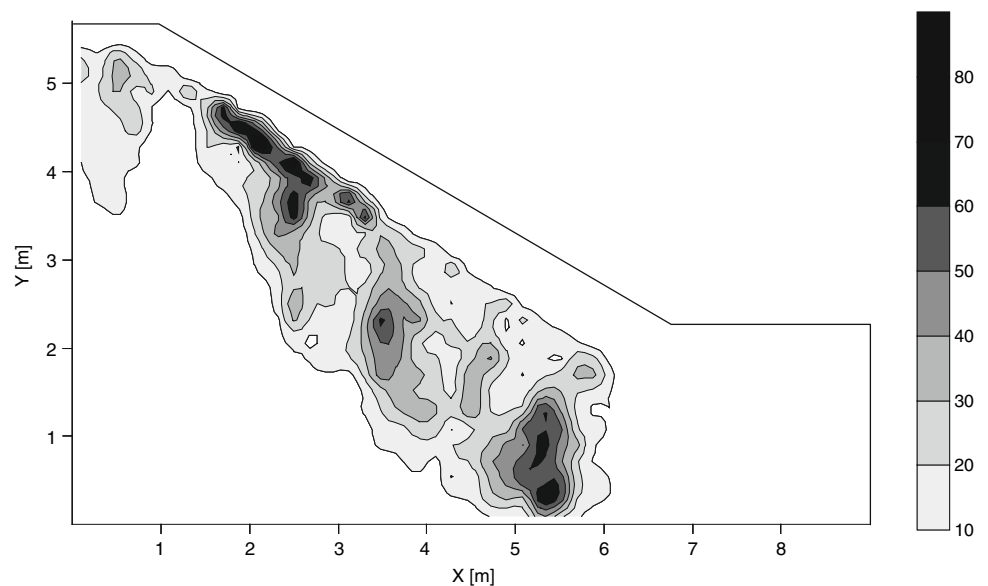
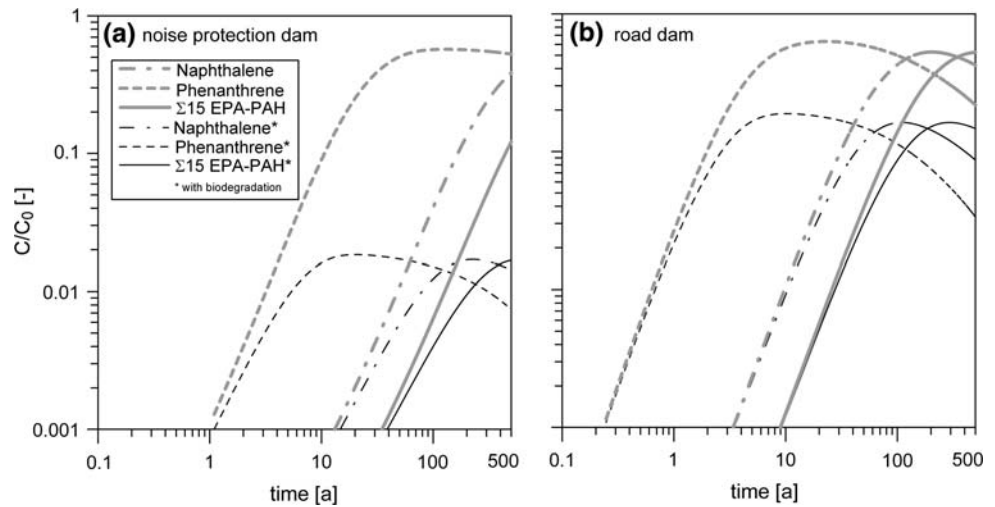


**Fig. 12** Breakthrough curves for the three contaminants: naphthalene, phenanthrene and the sum parameter  $\Sigma$  15EPA-PAH with (*thin black curves*) and without (*thick gray curves*) biodegradation at the groundwater surface below the noise protection dam (a) and the road dam (b). Concentrations are spatially averaged along the respective lower model boundaries



velocity at nodes can be different depending upon structured or unstructured elements. The RWPT model is also tested for transport for steady and transient velocity fields of flow in saturated/unsaturated porous media. The RWPT model produced the results in good agreement of the results obtained by the FEM.

In comparison with prior results (Hassan and Mohamed 2003) for advective and diffusive transport in homogeneous media, the proposed RWPT model successfully reduced the number of particles by about two orders of magnitude without losing the accuracy of the concentration contours. For the problem studied, simulations using different numbers of particles indicate that the deviation between the analytical and the numerical solutions decreases significantly when raising the number of particles from 1,000 to 10,000. A further increase in particle numbers yields only little additional accuracy.

Finally, the RWPT method was applied in a study on contaminant leaching under unsaturated conditions from demolition waste reused in two road constructions scenarios: a noise protection dam and a road dam. Travel time distributions of a passive tracer were calculated to characterize the hydraulics of the constructions, i.e. the spatial variability of unsaturated flow and transport patterns. Results from the RWPT method show good agreement when compared to simulations based on the Eulerian approach. It is found that due to the composite structure of the road constructions with strongly contrasting material properties capillary barriers develop along sloped material boundaries of the embankments. These capillary barriers cause large quantities of the seepage water to partially bypass the demolition waste. At the base of the embankments, however, infiltration into the demolition waste is focused resulting in high transport velocities especially for the road dam. As a consequence, also for sorbing or biodegradable contaminants' breakthrough of significant

concentrations to the groundwater surface might be possible within rather short time frames. These results suggest that the complex hydraulic behavior of road constructions should not be neglected in the assessment of the environmental impact of waste reuse in road base layers, as it has a relevant impact on contaminant leaching.

**References**

Ackerer P, Mose R, Siegel P, Chavent G (1996) Application of the mixed hybrid finite element approximation in a groundwater flow model: luxury or necessity? Reply. *Water Resour Res* 32(6):1911–1913

Bear J (1972) *Dynamics of fluids in porous media*. American Elsevier, New York, 761 p

Bear J (1979) *Hydraulics of groundwater*. McGraw-Hill, New York

Bensabat J, Zhou QL, Bear J (2000) An adaptive pathline-based particle tracking algorithm for the Eulerian-Lagrangian method. *Adv Water Resour* 23(4):383–397

Beyer C, Konrad W, Park CH, Bauer S, Rügner H, Liedl R, Grathwohl P (2007) Modellbasierte Sickerwasserprognose für die Verwertung von Recycling-Baustoffen in technischen Bauwerken. (Model based prognosis of contaminant leaching for reuse of demolition waste in construction projects). *Grundwasser* 12(2):94–107

Brezzi F, Fortin M (1991) *Mixed and hybrid finite elements methods*. Springer, New York

Chavent G, Roberts JE (1991) A unified physical presentation of mixed, mixed-hybrid finite elements and standard finite difference approximations for the determination of velocities in waterflow problems. *Adv Water Resour* 14(6):329–348

Cheng HP, Cheng JR, Yeh GT (1996) A particle tracking technique for the Lagrangian-Eulerian finite element method in multi-dimensions. *Int J Numer Methods Eng* 39(7):1115–1136

Cirpka OA, Frind EO, Helmig R (1999) Streamline-oriented grid generation for transport modelling in two-dimensional domains including wells. *Adv Water Resour* 22(7):697–710

Cordes C, Kinzelbach W (1992) Continuous groundwater velocity fields and path lines in linear, bilinear, and trilinear finite elements. *Water Resour Res* 28(11):2903–2911

Cordes C, Kinzelbach W (1996) Application of the mixed hybrid finite element approximation in a groundwater flow model:

- luxury or necessity? Comment. *Water Resour Res* 32(6):1905–1909
- Cortis A, Berkowitz B (2005) Anomalous transport in “classical” soil and sand columns. *Soil Sci Soc Am J* 69(1):285
- Delay F, Ackerer P, Danquigny C (2005) Simulating solute transport in porous or fractured formations using random walk particle tracking: a review. *Vadose Zone J* 4(2):360–379
- Durlofsky LJ (1994) Accuracy of mixed and control-volume finite-element approximations to Darcy velocity and related quantities. *Water Resour Res* 30(4):965–973
- Finkel M, Liedl R, Teutsch G (1999) Modelling surfactant-enhanced remediation of polycyclic aromatic hydrocarbons. *Environ Model Softw* 14(2–3):203–211
- Freeze RA, Cherry JA (1979) *Groundwater*. Prentice–Hall, Englewood Cliffs, 604 p
- Grathwohl P (1998) *Diffusion in natural porous media: contaminant transport, sorption/desorption and dissolution kinetics*, 224 S. Kluwer, Boston
- Haegland H (2003) *Streamline tracing in irregular grids*. Cand. Scient. Thesis, University of Bergen, Norway
- Haegland H, Dahle HK, Eigestad GT, Lie K-A, Aavatsmark I (2007) Improved streamlines and time-of-flight for streamline simulation on irregular grids. *Adv Water Resour* 30(4):1027–1045
- Hassan AE, Mohamed MM (2003) On using particle tracking methods to simulate transport in single-continuum and dual continua porous media. *J Hydrol* 275(3–4):242–260
- Hoteit H, Mose R, Younes A, Lehmann F, Ackerer P (2002) Three-dimensional modeling of mass transfer in porous media using the mixed hybrid finite elements and the random-walk methods. *Math Geol* 34(4):435–456
- Jang WY, Aral MM (2007) Density-driven transport of volatile organic compounds and its impact on contaminated groundwater plume evolution. *Transp Porous Media* 67(3):353–374
- Jury WA, Gardner WR, Gardner WH (1991) *Soil physics*. Wiley, New York, 328 p
- Kinzelbach W (1986) *Groundwater modelling: an introduction with sample programs in BASIC* Wolfgang Kinzelbach. Elsevier, Amsterdam
- Kolditz O, Wang W, Hesser J, Shao H, Du Y, Park C-H (2007a) Geosys/rockflow benchmarking. Center for Applied Geoscience, University of Tuebingen, GeoSys (Preprint)
- Kolditz O, Du Y, Bürger C, Delfs J, Kuntz D, Beinhorn M, Hess M, Wang W, van der Grift B, te Stroet C (2007b) Development of a regional hydrologic soil model and application to the Beerze-Reusel drainage basin. *Environ Pollut* (in press)
- LaBolle EM, Fogg GE, Tompson AFB (1996) Random-walk simulation of transport in heterogeneous porous media: local mass-conservation problem and implementation methods. *Water Resour Res* 32(3):583–593
- Matringe SF, Juanes R, Tchelepi HA (2006) Robust streamline tracing for the simulation of porous media flow on general triangular and quadrilateral grids. *J Comput Phys* 219(2):992–1012
- Mayer KU, Benner SG, Blowes DW, Frind EO (1999) The reactive transport model MIN3P: application to acid mine drainage generation and treatment—Nickel Rim Mine site, Sudbury, Ontario, vol 1. In: *Conference on mining and the environment*, pp 145–154
- Mose R, Siegel P, Ackerer P, Chavent G (1994) Application of the mixed hybrid finite-element approximation in a groundwater-flow model—luxury or necessity. *Water Resour Res* 30(11):3001–3012
- Ogata A, Banks RB (1961) *A solution of the differential equation of longitudinal dispersion in porous media; fluid movement in earth materials*. US Govt Print Off, Washington
- Oliveira A, Baptista AM (1998) On the role of tracking on Eulerian-Lagrangian solutions of the transport equation. *Adv Water Resour* 21(7):539–554
- Park C-H, Aral MM (2007) Sensitivity of the solution of the Elder problem to density, velocity and numerical perturbations. *J Contam Hydrol* 92:33–49
- Park C-H, Beyer C, Bauer S, Kolditz O (2007) Benchmark test for random walk particle tracking methods. Center for Applied Geoscience, University of Tuebingen, GeoSys (Preprint)
- Pollock DW (1988) Semianalytical computation of path lines for finite-difference models. *Ground Water* 26(6):743–750
- Prevost M (2000) *The streamline method for unstructured grids*. MS, Stanford University, USA
- Prevost M, Edwards MG, Blunt MJ (2002) Streamline tracing on curvilinear structured and unstructured grids. *SPE J* 7(2):139–148
- Salamon P, Fernandez-Garcia D, Gomez-Hernandez JJ (2006) A review and numerical assessment of the random walk particle tracking method. *J Contam Hydrol* 87(3–4):277–305
- Tompson AFB, Gelhar LW (1990) Numerical-simulation of solute transport in 3-dimensional, randomly heterogeneous porous-media. *Water Resour Res* 26(10):2541–2562
- Šimůnek J, van Genuchten MT, Šejna M (2005) *The Hydrus-1d software package for simulating the one-dimensional movement of water, heat, and multiple solutes in variably-saturated media, version 3.0*. Technical Report. Department of Environmental Science, University of California Riverside
- Warrick AW, Biggar JW, Nielsen DR (1971) Simultaneous solute and water transfer for an unsaturated soil. *Water Resour Res* 7:1216–1225
- Yeh GT (1981) On the computation of darcian velocity and mass balance in the finite-element modeling of groundwater-flow. *Water Resour Res* 17(5):1529–1534